Polarised Study of Diboson Production at NNLO

Andrei Popescu
in collaboration with Rene Poncelet
based on [Poncelet, AP 2102.13583]

`popescu@hep.phy.cam.ac.uk`

Cavendish Laboratory, University of Cambridge

XII Lomonosov Conference

`https://lomcon.ru`
Moscow State University

Tuesday 24$^{\text{th}}$ August, 2021

Outline of the talk

1. **QCD Precision Studies**
   - Cross section at hadron collider
2. **Process**
   - Motivation
   - Aspects of diboson production
   - Double-pole approximation
3. **Calculation**
   - Setup
   - NNLO corrections
   - Loop-induced channel corrections
   - Polarisation fractions
4. **Conclusions**
   - Future plans

QCD Precision Studies

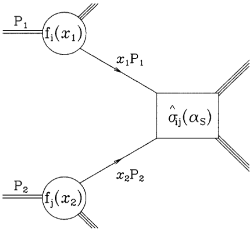

Figure 1: Parton model description of a hard scattering process (Ellis, Stirling, Webber).

Master formula for collinear factorisation:

$$\sigma(P_1, P_2) = \sum_{i,j} \int dx_1\, dx_2 \cdot \underbrace{f_i(x_1, \mu_F^2) \cdot f_j(x_2, \mu_F^2)}_{\text{Parton distribution functions (PDF)}} \cdot \underbrace{\hat{\sigma}_{ij}}_{\text{Partonic cross-section}} \left(x_1 P_1, x_2 P_2, \alpha_s(\underbrace{\mu_R^2}_{\text{Renormalisation scale}}), \mu_R^2, \underbrace{\mu_F^2}_{\text{Factorisation scale}} \right) .$$

Parton distribution functions (PDF)

Renormalisation scale

Partonic cross-section

Factorisation scale

Splitting function

DGLAP equation for PDF evolution

$$\mu \frac{d}{d\mu} f_i(x, \mu) = \frac{\alpha_s}{\pi} \int_x^1 \frac{d\xi}{\xi} f_i(\xi, \mu) \cdot P_{qq} \left(\frac{x}{\xi} \right) .$$

Perturbative expansion in powers of α_S

$$\hat{\sigma}_{ij} = \hat{\sigma}_{ij}^{(0)} + \hat{\sigma}_{ij}^{(1)} + \hat{\sigma}_{ij}^{(2)} + \ldots$$

The difficulty comes not from UV but IR divergencies.

Example with quark production (final state radiation):

Born $(M_n^{(0)})$

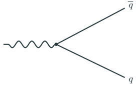

Real emission $(M_{n+1}^{(0)})$

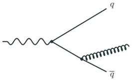

Virtual loop $(M_n^{(1)})$

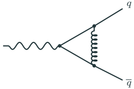

Double virtual $(M_n^{(2)})$

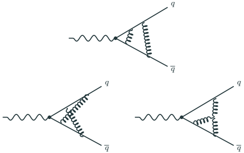

Real-virtual $(M_{n+1}^{(1)})$

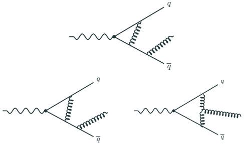

Double real $(M_{n+2}^{(0)})$

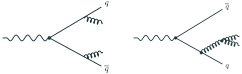

Kinoshita-Lee-Neuberger theorem

Regularised virtual poles cancel against real radiation singularities upon inclusive integration of the emission phase space.

Perturbative expansion for σ_{ab} :

$$\hat{\sigma}_{ab}^{(0)} \sim \int d\Phi_n \left\langle M_n^{(0)} \middle| M_n^{(0)} \right\rangle F_n \qquad \hat{\sigma}_{ab}^{(1)} \sim \int d\Phi_{n+1} \left\langle M_{n+1}^{(0)} \middle| M_{n+1}^{(0)} \right\rangle F_{n+1} + 2 \int d\Phi_n \,\mathrm{Re} \left\langle M_n^{(0)} \middle| M_n^{(1)} \right\rangle F_n$$

$$\hat{\sigma}_{ab}^{(2)} \sim \int d\Phi_{n+2} \left\langle M_{n+2}^{(0)} \middle| M_{n+2}^{(0)} \right\rangle F_{n+2} + 2 \int d\Phi_n \,\mathrm{Re} \left\langle M_n^{(0)} \middle| M_{n+1}^{(2)} \right\rangle F_n + \int d\Phi_{n+1} \left\langle M_{n+1}^{(1)} \middle| M_{n+1}^{(1)} \right\rangle F_{n+1}$$

Benefits:

- Significant reduction of scale uncertainty (to 1% at NNLO)

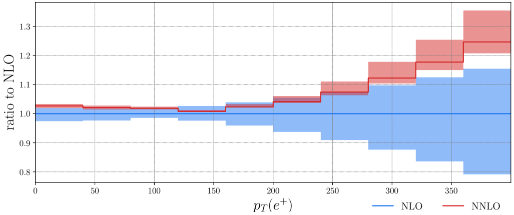

Challenges:

- Computational complexity (100-1000x compared to NLO)
- Some schemes tackle only a subset of processes

Fact

It took a long time to establish NNLO precision as standard:
2-loop amplitudes for dijet process were available 20 years before cross-section prediction arrived.

Theoretical uncertainty is estimated through "7-point scale variation"

$$\tfrac{1}{2} < \mu_R, \mu_F < 2.$$

Common differential observables:

- rapidity ($y = \frac{1}{2} \ln \left(\frac{E+p_z}{E-p_z} \right)$)
- transverse momentum (p_T)
- invariant masses
- distance between particles $dR = \sqrt{y^2 + \Delta\phi^2}$
- event shapes (thrust, N-jettiness, ...): to describe geometry of a group of particles

Benefits:

- Significant reduction of scale uncertainty (to 1% at NNLO)

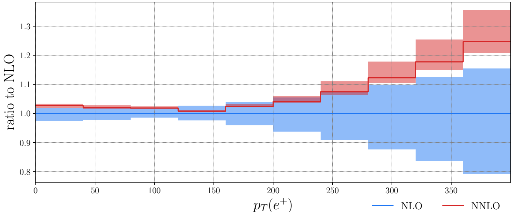

Challenges:

- Computational complexity (100-1000x compared to NLO)
- Some schemes tackle only a subset of processes

Fact

It took a long time to establish NNLO precision as standard:
2-loop amplitudes for dijet process were available 20 years before cross-section prediction arrived.

Theoretical uncertainty is estimated through "7-point scale variation"

$$\frac{1}{2} < \mu_R, \mu_F < 2.$$

"Sector-improved residue subtraction scheme"

Project leader Michal Czakon [1005.0274, 1408.2500]

Contributors Arnd Behring, David Heymes, Alexander Mitov, Andrew Papanastasiou, Mathieu Pellen, Rene Poncelet, *A.P.*

Features
- local numerical cancellation of poles
- versatile scheme: any process possible
- implemented in C++ library STRIPPER

Processes
- $t\bar{t}$ [1901.05407, 2008.11133] ,
- dijet [1907.12911] ,
- 3-photon [1911.00479] ,
- V+c [2011.01011] ,
- 2-photon+jet [2105.06940] ,
- 3-jet [2106.05331] .

Process

Polarised diboson production: *overview*

Longitudinal polarisation and massiveness of $W^{\pm}, Z$ bosons is the direct consequence of the Electroweak symmetry breaking mechanism in the Standard Model.

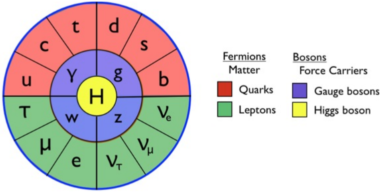

Features of $pp \to W^+W^- \to e^+\nu_e\mu^-\overline{\nu}_\mu$:

- Leptonic decay channel
  is a clean experimental signature
- Largest σ among diboson processes
- Luminosities of Run 2/3
  will allow for precise measurement

Relevant theoretical papers:

- Seminal papers on W-boson polarisation
  [Bern et al. 1103.5445]
  [Stirling et al. 1204.6427]
- Polarised diboson production at NLO QCD
  [Denner et al. 2006.14867, 2010.07149]
- Double pole approximation (DPA)
  [Billoni et al. 1310.1564]
  [Ballestrero et al. 1710.09339, 1907.04722]
- Off-shell W^+W^- production up to NNLO QCD + EW NLO
  [Caola et al. 1511.08617]
  [Grazzini et al. 1605.02716, 1912.00068]
  [Lombardi et al. 2103.12077]

Polarised diboson production: *technical aspects*

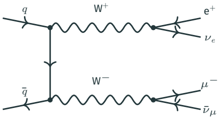

Double resonant (DR)

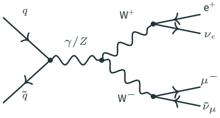

Double resonant (DR)

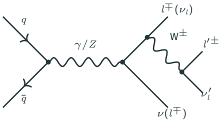

Single resonant (SR)

1. *On-shell amplitudes:*
   - → **polarisation** is defined for **on-shell** bosons;
   - → **non-resonant background** effects due to missing SR amplitudes;
   - → accuracy is $\sim \mathcal{O}(\Gamma_W/M_W) = 2.5\%$;

Polarised diboson production: *technical aspects*

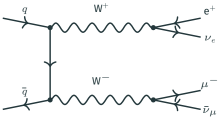

Double resonant (DR)

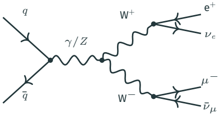

Double resonant (DR)

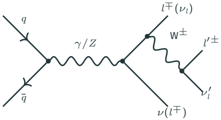

Single resonant (SR)

1. *On-shell amplitudes:*
   - → **polarisation** is defined for **on-shell** bosons;
   - → **non-resonant background** effects due to missing SR amplitudes;
   - → accuracy is $\sim \mathcal{O}(\Gamma_W / M_W) = 2.5\%$;
2. *Interference between polarisations:*
   - → caused by **cross terms** $\mathcal{A}^*_\lambda \mathcal{A}_{\lambda'}$ (polarisation information lost after leptonic decay);
   - → arises if **leptonic phase space integration** is restricted (fiducial setup or specific observable);
   - → problematic for experiment (polarisation measurement based on template method).

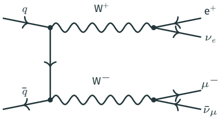

Double resonant (DR)

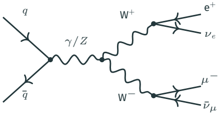

Double resonant (DR)

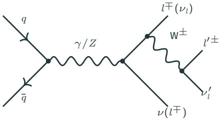

Single resonant (SR)

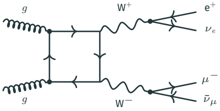

Loop-induced (LI)

1. *On-shell amplitudes:*
   - → **polarisation** is defined for **on-shell** bosons;
   - → **non-resonant background** effects due to missing SR amplitudes;
   - → accuracy is $\sim \mathcal{O}(\Gamma_W/M_W) = 2.5\%$;
2. *Interference between polarisations:*
   - → caused by **cross terms** $\mathcal{A}^*_\lambda \mathcal{A}_{\lambda'}$ (polarisation information lost after leptonic decay);
   - → arises if **leptonic phase space integration** is restricted (fiducial setup or specific observable);
   - → problematic for experiment (polarisation measurement based on template method).
3. *Loop-induced channel:*
   - → significant effects and **dominating** scale uncertainty at $\mathcal{O}(\alpha_s^2)$.

Method: Double-pole approximation

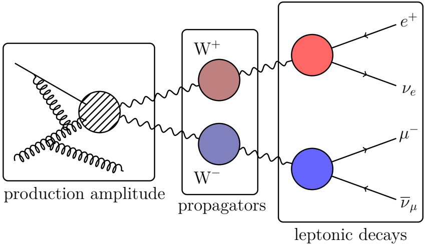

Full amplitude is approximated by **on-shell sub-amplitudes** and the **off-shell propagators**:

$$A \approx \sum_{\alpha,\beta} A^{pp\to W^+W^-}_{\alpha\beta,\mu\nu} \frac{A^\mu_\alpha(W^+ \to l^+\nu)\cdot A^\nu_\beta(W^- \to l^-\overline{\nu})}{(p_+^2 - M^2)\cdot(p_-^2 - M^2)},$$

boson polarisations

- A selected **on-shell projection** defined on-shell sub-amplitudes *(we choose to preserve leptonic angles in the decay frames, and boson angles in the diboson frame).*
- Cross-term amplitude contributions coming from $A_\alpha A_{\tilde{\alpha}}$ terms create **interferences** for cross sections.

Calculation

Setup

Process: $pp \to W^+W^- \to e^+\nu_e\mu^-\overline{\nu}_\mu$ @ 13 TeV.

Details: Massive b-quarks scheme (*Nf=4*), G_μ-scheme, complex-mass scheme.

PDF sets: `NNPDF31_[n]nlo_as_0118` (*5-flavour*).

Scales: fixed central scale $\mu_R = \mu_F = M_W$,
7-point variation scheme with $1/2 \leq \mu_R/\mu_F \leq 2$.

Cuts: ATLAS-inspired[1] fiducial setup:

$p_{T\,miss} > 20$ GeV	to avoid D-Y background
$M_{e^+\mu^-} > 55$ GeV	to avoid Higgs background
perfect b-quark jet veto	to avoid $t\bar{t}$ background
$p_{T,l} > 27$ GeV, $\|y_l\| < 2.5$	detector cuts
jet veto: $\|\eta_j\| < 4.5$, $p_{T,j} > 35$ GeV	to reduce QCD corrections

Finally, an **implicit cut** on $M_{\mathrm{W}^+,\mathrm{W}^-} > 2M_{\mathrm{W}}$ comes from double resonant parts in DPA, NWA.

[1] [Aaboud et al. 1902.05759]

Distribution at NNLO

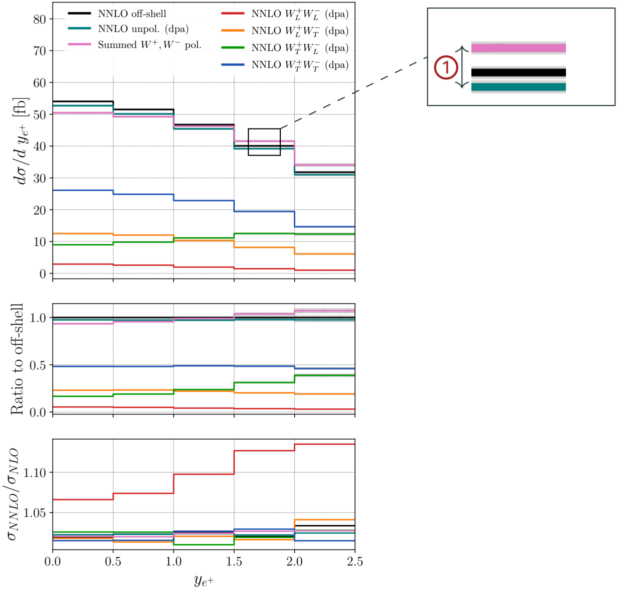

Features:

1. Polarisation interference

Distribution at NNLO

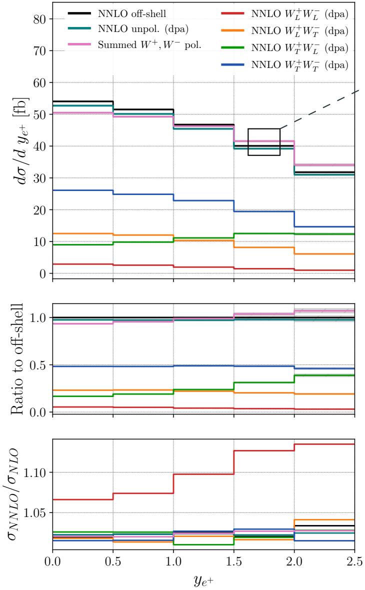

Features:

1. Polarisation interference
2. Non-resonant background

Distribution at NNLO

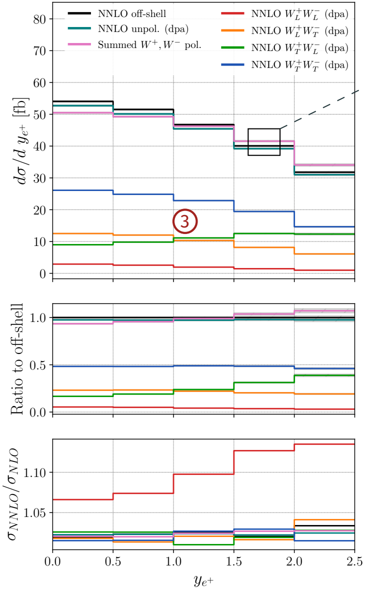

Features:

1. Polarisation interference
2. Non-resonant background
3. ”Monte-Carlo true” polarisation distributions

Distribution at NNLO

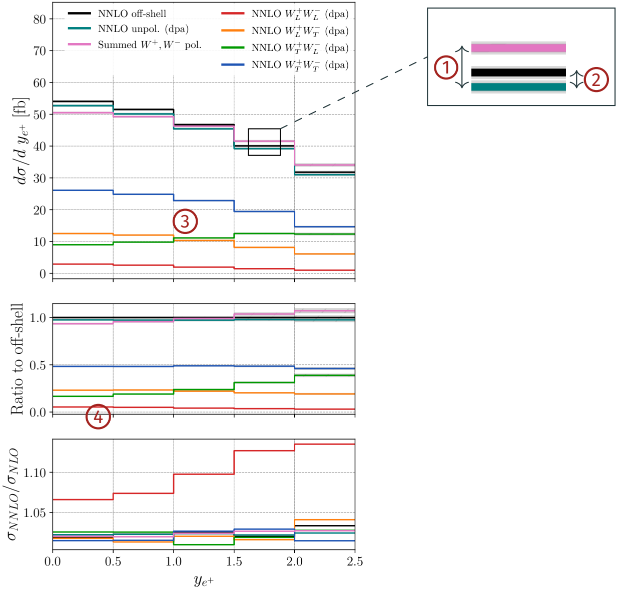

Features:

1. Polarisation interference
2. Non-resonant background
3. ”Monte-Carlo true” polarisation distributions
4. $W^+_L W^-_L$ contribution is small,
   $W^+_T W^-_T$ dominates

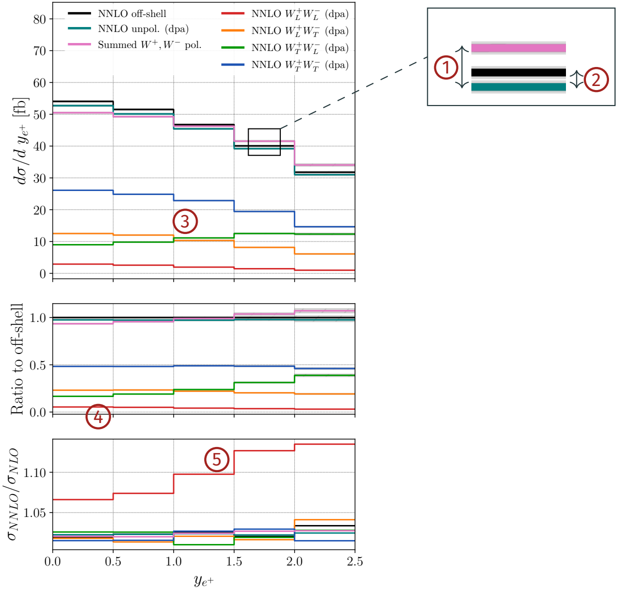

Features:

1. Polarisation interference
2. Non-resonant background
3. "Monte-Carlo true" polarisation distributions
4. $W_L^+ W_L^-$ contribution is small, $W_T^+ W_T^-$ dominates
5. Distinct and large K_{NNLO} for $W_L^+ W_L^-$

Distribution at NNLO

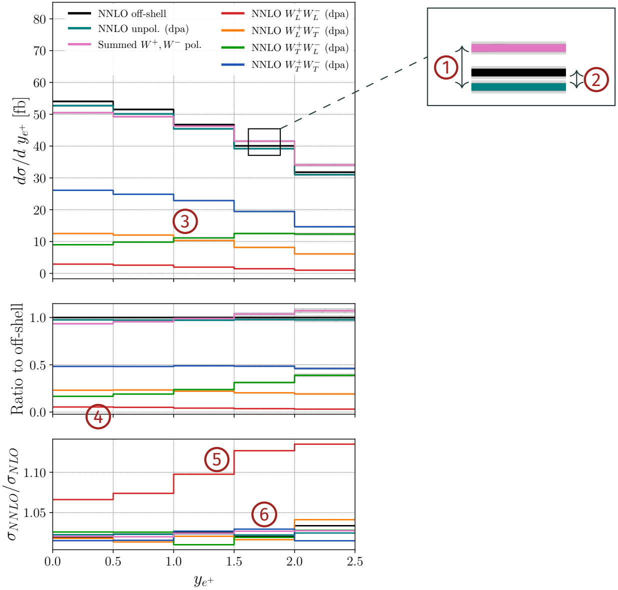

Features:

1. Polarisation interference
2. Non-resonant background
3. "Monte-Carlo true" polarisation distributions
4. $W_L^+ W_L^-$ contribution is small, $W_T^+ W_T^-$ dominates
5. Distinct and large K_{NNLO} for $W_L^+ W_L^-$
6. small K-factor for other setups

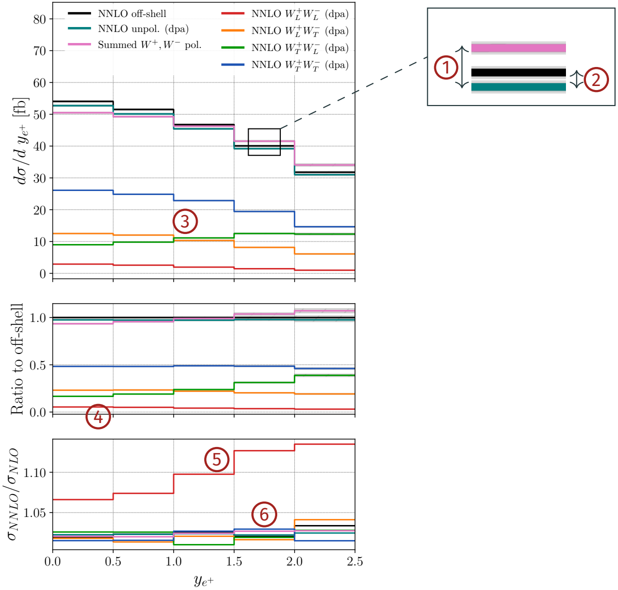

Features:

1. Polarisation interference
2. Non-resonant background
3. "Monte-Carlo true" polarisation distributions
4. $W_L^+ W_L^-$ contribution is small, $W_T^+ W_T^-$ dominates
5. Distinct and large K_{NNLO} for $W_L^+ W_L^-$
6. small K-factor for other setups

Summary:

- → NNLO effects are **2-3%** of σ_{tot} for all setups except $W_L^+ W_L^-$ where it is **9%.**
- → Scale uncertainty is reduced by a **factor of 3** w.r.t NLO.

Loop-induced channel effects

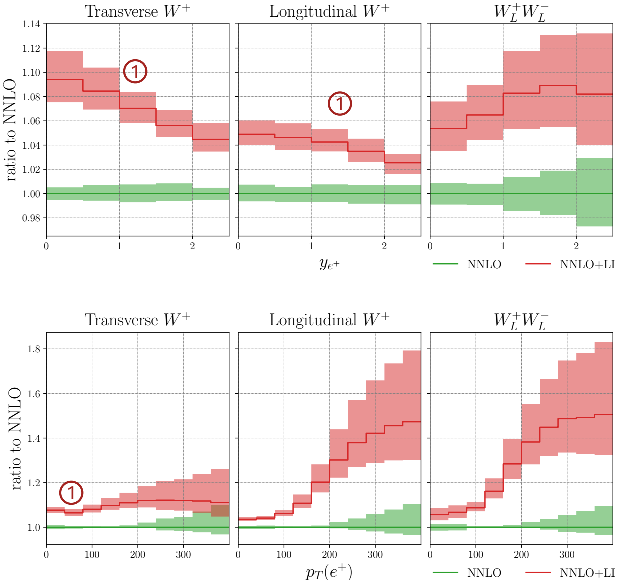

Selected effects

1. Larger corrections for W_T at low energies

Loop-induced channel effects

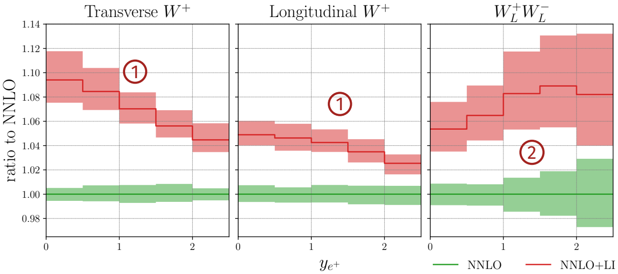

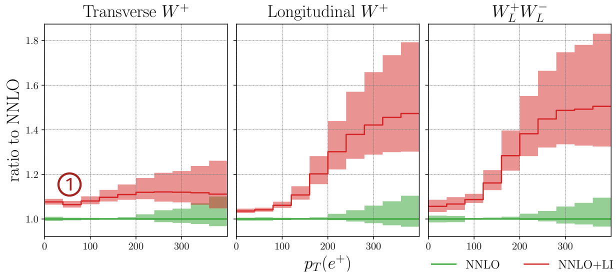

Selected effects

1. Larger corrections for W_T at low energies
2. Distinct rapidity correction profile for $W_L^+ W_L^-$

Loop-induced channel effects

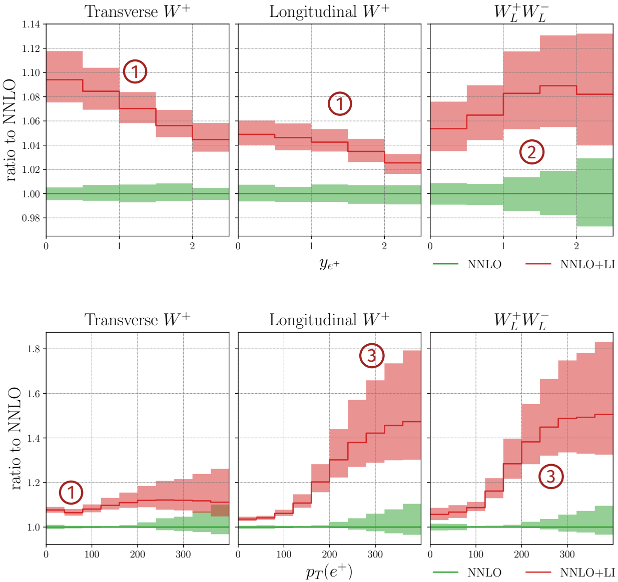

Selected effects

1. Larger corrections for W_T at low energies
2. Distinct rapidity correction profile for $W_L^+ W_L^-$
3. Massive high-energy corrections for longitudinal W, matching bahaviour in $W_L^+ W_L^-$

Loop-induced channel effects

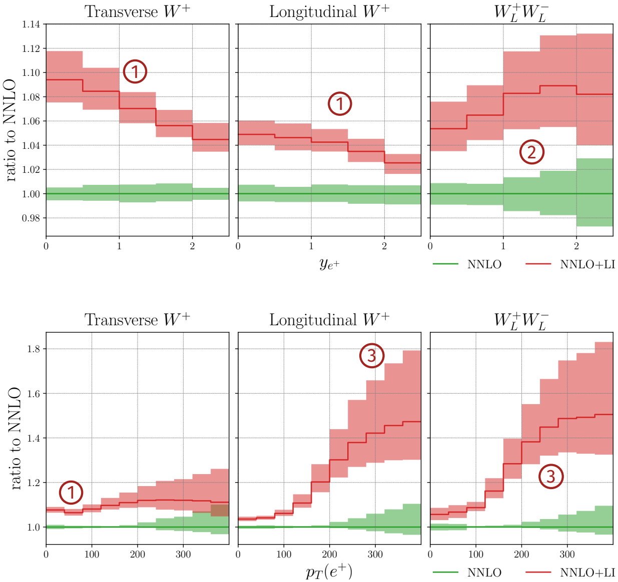

Selected effects

1. Larger corrections for W_T at low energies
2. Distinct rapidity correction profile for $W_L^+W_L^-$
3. Massive high-energy corrections for longitudinal W, matching bahaviour in $W_L^+W_L^-$

Summary:

→ Corrections of 6-9% to σ_{tot}.

→ Overall scale uncertainty increased by a factor of 2.

→ Correction profile does not follow NNLO K-factor.

In our fiducial setup, interferences are small ($2 - 3\%$), allowing for polarisation fraction extraction:

$$f_i = \frac{\sigma_i}{\sigma_{tot}}.$$

- $W_L^+ W_L^-$ setup is significantly affected by NNLO corrections, others are stable;
- Loop-induced channel affects $W_T^+ W_T^-$ setup the most.

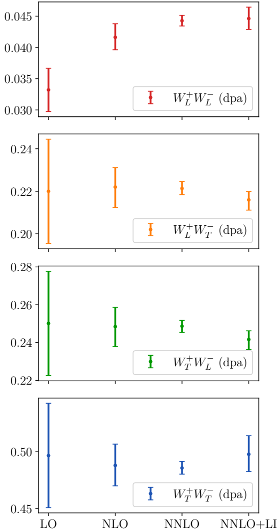

Figure 4: Polarisation fractions (errorbars defined by scale uncertainties).

Conclusions

We studied W-boson polarisation in the fully leptonic channel of $pp \to W^+W^-$ process.

Polarisations were separated on the amplitude level in the framework of DPA.

- **NNLO corrections** bring scale uncertainty down to 1% and are **well-behaved**.
- QCD corrections are polarisation dependent and are particularly strong for the **doubly-longitudinal** setup.
- **Loop-induced** channel has a $6-9\%$ effect on the results and increases scale uncertainty by a factor of 2.

Future plans:

- Calculate NLO corrections to LI channel in diboson production.
- Study polarised $W + j$ process at NNLO.

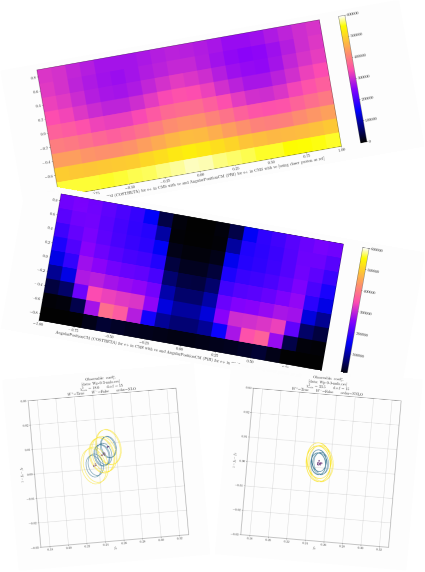

From polarised study of $W + j$ at NNLO
[in preparation]

Future plans:

- Calculate NLO corrections to LI channel in diboson production.
- Study polarised $W + j$ process at NNLO.

Thank you for your attention!

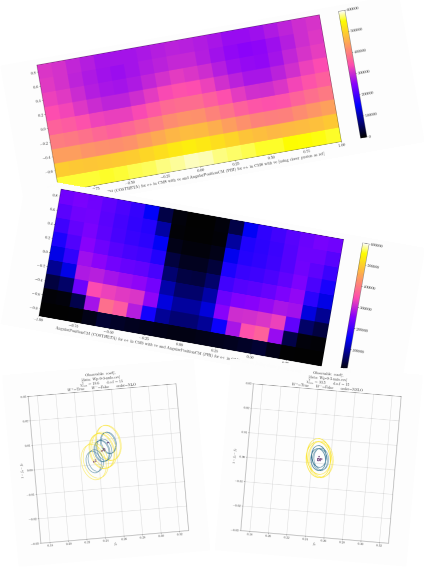

From polarised study of $W + j$ at NNLO
[in preparation]

Backup

Tools

- STRIPPER: general purpose framework for fixed-order calculations up to NNLO QCD.
  [Czakon et al. 1907.12911, 1408.2500]
- AVH: tree-level amplitudes.
  [Bury, van Hameren 1503.08612]
- OPENLOOPS: 1-loop amplitudes (privately modified for polarised study).
  [Buccioni et al. 1907.13071, 1710.11452] [Cascioli et al. 1111.5206]
- RECOLA: checks in 1-loop amplitudes (private version used by authors of the NLO study).
  [Actis et al. 1211.6316, 1605.01090]
- VVAMP: 2-loop amplitudes for $q\,\overline{q}$ channel.
  [Gehrmann et al. 1503.04812]
- LHAPDF: particle distribution functions framework.
  [Buckley et al. 1412.7420]

Fixed-order calculation schemes (NNLO)

Brief look at competing schemes:

- Slicing method:
  - resummation formulae are used to approximate divergent phase-space regions within a small cutoff;
  - q_T **subtraction** (MATRIX code) and **N-jettiness** use corresponding observables as cut-off variables;
  - used for diboson and boson+jet production;
- Subtraction method:
  - Fully differential subtraction with numerically integrated subtraction terms;
  - **Antenna subtraction** first used as NLO scheme, promoted to NNLO;
  - **CoLoRFulNNLO** developed for colourless initial states;
  - **Local analytic sector subtraction** with analytic counterterms;
  - used for *e.g.* 2-jet, V+j, $t\bar{t}$, $e^+e^- \to 3$j.

"Sector-improved residue subtraction scheme"

Project leader Michal Czakon [1005.0274, 1408.2500]

Contributors Arnd Behring, David Heymes, Alexander Mitov, Andrew Papanastasiou, Mathieu Pellen, Rene Poncelet, *A.P.*

Features
- local numerical cancellation of poles
- versatile scheme: any process possible
- implemented in C++ library STRIPPER

Processes
- $t\bar{t}$ [1901.05407, 2008.11133] ,
- dijet [1907.12911] ,
- 3-photon [1911.00479] ,
- V+c [2011.01011] ,
- 2-photon+jet [2105.06940] ,
- 3-jet [2106.05331] .

Polarised Weak bosons: amplitude

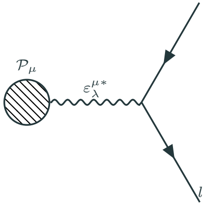

Double pole approximation:

$$\mathcal{A}_\lambda = \mathcal{P}_\mu \frac{\varepsilon_\lambda^\mu \varepsilon_\lambda^{\nu *}}{k^2 - M_V^2 + iM_V\Gamma_V} \mathcal{D}_\nu$$

$$\mathcal{M} = \sum_\lambda |A_\lambda|^2 + \sum_{\lambda \neq \lambda'} A_\lambda^* A_{\lambda'}$$

Polarisation only defined for physical vectors (present physical vectors), so define on-shell projection (OSP) for kinematics and evaluate $\mathcal{P}, \mathcal{D}$ at this point.
Narrow width approximation:

$$\mathcal{M}_{\mathrm{pp}\to\mathrm{e}^+\nu_\mathrm{e}\mu^-\bar{\nu}_\mu} \sim \sum_{h,h' \in \Lambda} \mathcal{M}^{h,h'}_{\mathrm{pp}\to\mathrm{W}^+\mathrm{W}^-} \Gamma^h_{\mathrm{W}^+\to\mathrm{e}^+\nu_\mathrm{e}} \Gamma^{h'}_{\mathrm{W}^-\to\mu^-\bar{\nu}_\mu},$$

Precision of a method that uses on-shell amplitudes is of $\mathcal{O}(\Gamma_W/M_W)$ for inclusive computation.

Beware of interference terms in the unpolarised case:

$$|M|^2 = \sum_\lambda |M_\lambda|^2 + \sum_{\lambda \neq \lambda'} M_\lambda^* M_{\lambda'}$$

Polarised Weak boson: cross-section

Analytic result for polarised massive vector boson decay in its CM frame:

$$\frac{1}{\sigma}\frac{d^2\sigma}{d\cos\theta^*\, d\phi^*} = \frac{3}{16\pi}\Big[(1+\cos^2\theta^*) + A_0\frac{1}{2}(1-3\cos^2\theta) + A_1\sin(2\theta^*)\cos\phi^* + A_2\frac{1}{2}\sin^2\theta^*\cos(2\phi^*)$$
$$+ A_3\sin\theta^*\cos\phi^* + A_4\cos\theta^* + A_5\sin^2\theta^*\sin(2\phi^*) + A_6\sin(2\theta^*)\sin\phi^* + A_7\sin\theta^*\sin\phi^*\Big]$$

(coefficients depend on the choice of a coordinate system, e.g ”helicity”, ”Collins-Soper”, etc)
In case of inclusive phase space azimuthal angle can be integrated out:

$$\frac{1}{\sigma}\frac{d\sigma}{d(\cos\theta^*)} = \frac{3}{8}(1\mp\cos\theta^*)^2 f_- + \frac{3}{8}(1\pm\cos\theta^*)^2 f_+ + \frac{3}{4}\sin^2\theta^* f_L$$

where

$$f_\pm = \frac{1}{4}(2 - A_0 \pm A_4), \qquad f_0 = \frac{1}{2}A_0.$$

or through angular measurements:

$$f_\pm = -\frac{1}{2} \pm \langle\cos\theta^*\rangle + \frac{5}{2}\langle\cos^2\theta^*\rangle, \qquad f_0 = 2 - 5\langle\cos^2\theta^*\rangle.$$

DPA vs NWA: *total cross section*

	$\frac{\sigma_{NLO}}{\sigma_{LO}}$	$\frac{\sigma_{NNLO}}{\sigma_{NLO}}$	NNLO+LI [fb]	$\frac{\sigma_{NNLO+LI}}{\sigma_{NLO}}$
unpol. (dpa)	1.095	1.023	$232.7(4)^{+1.4\%}_{-1.1\%}$	1.061
unpol. (nwa)	1.097	1.025	$241.0(6)^{+1.5\%}_{-1.1\%}$	1.060

Features:

DPA vs NWA: *positron emission angle*

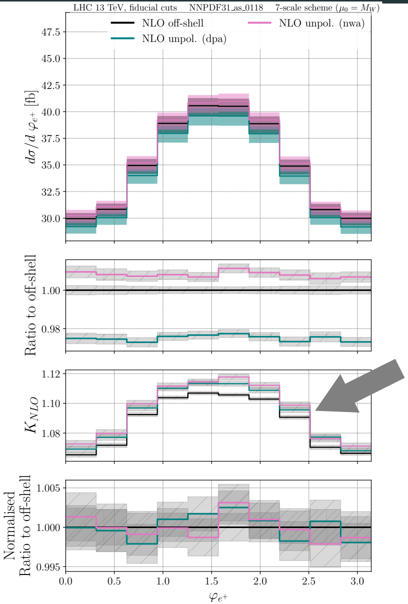

	$\frac{\sigma_{NLO}}{\sigma_{LO}}$	$\frac{\sigma_{NNLO}}{\sigma_{NLO}}$	NNLO+LI [fb]	$\frac{\sigma_{NNLO+LI}}{\sigma_{NLO}}$
unpol. (dpa)	1.095	1.023	$232.7(4)^{+1.4\%}_{-1.1\%}$	1.061
unpol. (nwa)	1.097	1.025	$241.0(6)^{+1.5\%}_{-1.1\%}$	1.060

Features:

- Close K-factors for all QCD corrections.

DPA vs NWA: *positron emission angle*

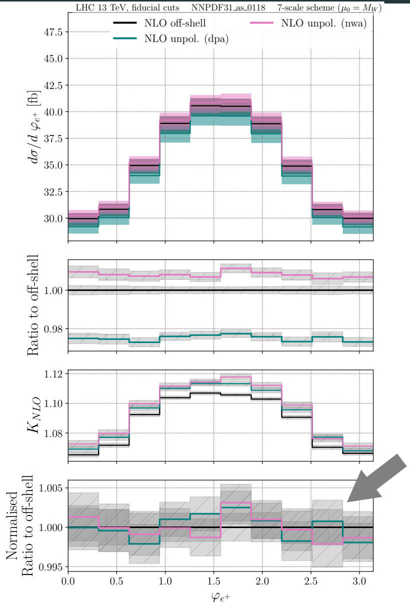

	$\frac{\sigma_{NLO}}{\sigma_{LO}}$	$\frac{\sigma_{NNLO}}{\sigma_{NLO}}$	NNLO+LI [fb]	$\frac{\sigma_{NNLO+LI}}{\sigma_{NLO}}$
unpol. (dpa)	1.095	1.023	$232.7(4)^{+1.4\%}_{-1.1\%}$	1.061
unpol. (nwa)	1.097	1.025	$241.0(6)^{+1.5\%}_{-1.1\%}$	1.060

Features:

- Close K-factors for all QCD corrections.
- Matching description of normalised bulk-defined distributions between DPA & NWA.

DPA vs NWA: *leading lepton transverse momentum*

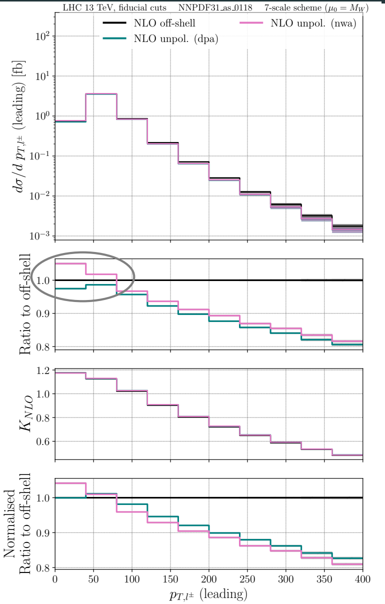

	$\frac{\sigma_{NLO}}{\sigma_{LO}}$	$\frac{\sigma_{NNLO}}{\sigma_{NLO}}$	NNLO+LI [fb]	$\frac{\sigma_{NNLO+LI}}{\sigma_{NLO}}$
unpol. (dpa)	1.095	1.023	$232.7(4)^{+1.4\%}_{-1.1\%}$	1.061
unpol. (nwa)	1.097	1.025	$241.0(6)^{+1.5\%}_{-1.1\%}$	1.060

Features:

- Close K-factors for all QCD corrections.
- Matching description of normalised bulk-defined distributions between DPA & NWA.
- Differences come from the bulk region.

DPA vs NWA: *azimuthal angle between leptons*

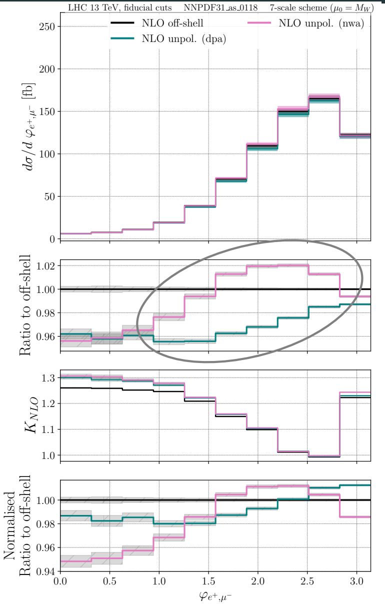

	$\frac{\sigma_{NLO}}{\sigma_{LO}}$	$\frac{\sigma_{NNLO}}{\sigma_{NLO}}$	NNLO+LI [fb]	$\frac{\sigma_{NNLO+LI}}{\sigma_{NLO}}$
unpol. (dpa)	1.095	1.023	$232.7(4)^{+1.4\%}_{-1.1\%}$	1.061
unpol. (nwa)	1.097	1.025	$241.0(6)^{+1.5\%}_{-1.1\%}$	1.060

Features:

- Close K-factors for all QCD corrections.
- Matching description of normalised bulk-defined distributions between DPA & NWA.
- Differences come from the bulk region.
- Interesting interplay in azimuthal angle.

DPA vs NWA

	$\frac{\sigma_{NLO}}{\sigma_{LO}}$	$\frac{\sigma_{NNLO}}{\sigma_{NLO}}$	NNLO+LI [fb]	$\frac{\sigma_{NNLO+LI}}{\sigma_{NLO}}$
unpol. (dpa)	1.095	1.023	$232.7(4)^{+1.4\%}_{-1.1\%}$	1.061
unpol. (nwa)	1.097	1.025	$241.0(6)^{+1.5\%}_{-1.1\%}$	1.060

Features:

- Close K-factors for all QCD corrections.
- Matching description of normalised bulk-defined distributions between DPA & NWA.
- Differences come from the bulk region.
- Interesting interplay in azimuthal angle.

$\Longrightarrow$ Overall **good description** of differential distributions **by NWA**.

Top-quark loop contribution in LI channel: off-shell setup

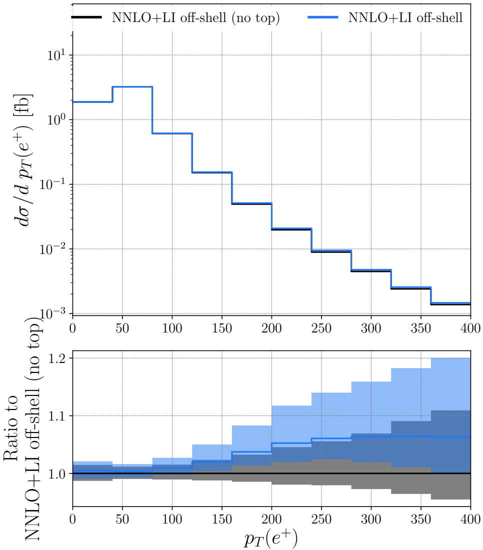

- Main effect in the tail:
  → value increase by up to 8%
  → scale variation band increased by 30%
- Effect on total cross section:
  → cross section increased by 0.6%
  → scale uncertainty increased by 7%

Top-quark loop contribution in LI channel: bulk observable

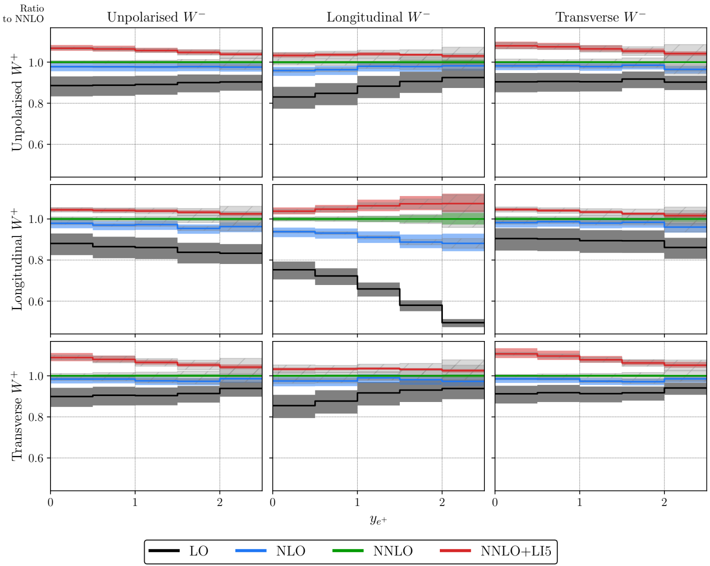

No significant effect on bulk observables from top-quark loop.

Effects of the PDF set

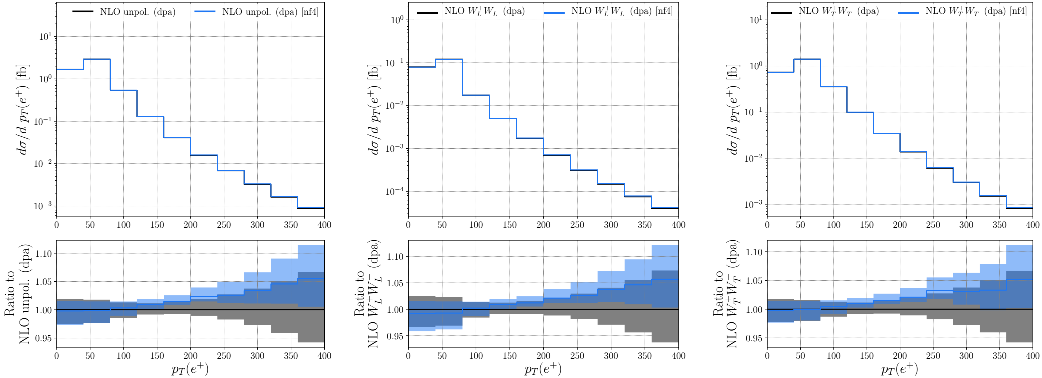

Figure 5: Comparison between calculations with $nf = 4$ and $nf = 5$ PDF sets. Uncertainty bands correspond to **factorisation** scale uncertainty.

- the discrepancy falls withing this band at NLO;
- total cross-section effect: $< 0.6\%$ (largest for LL).

Distribution poorly suited for polarisation study

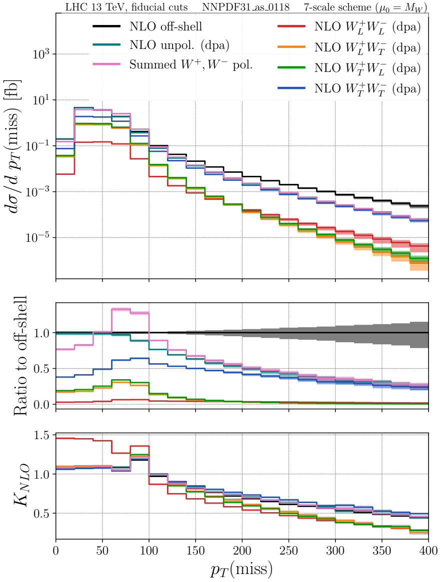

Single resonant contributions are dominating at high $p_{T,\text{miss}}$.

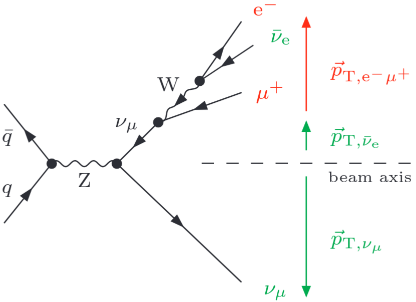

Figure 6: Dominating single resonant contribution at high p_T [Biedermann et al. 1605.03419]

Extra figures: M_{e^+,μ^-}

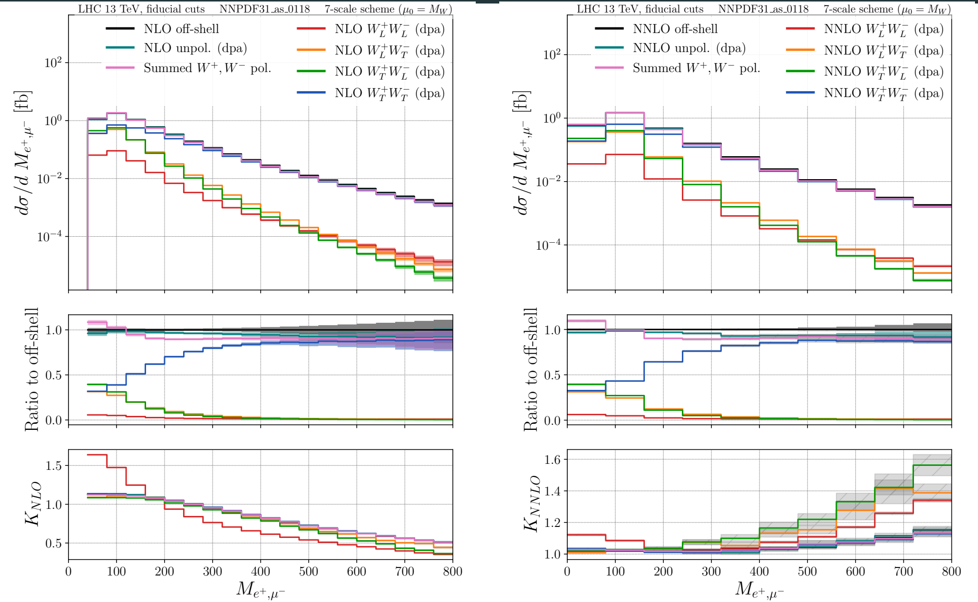

Extra figures: $\cos\theta_{e^+,\mu^-}$

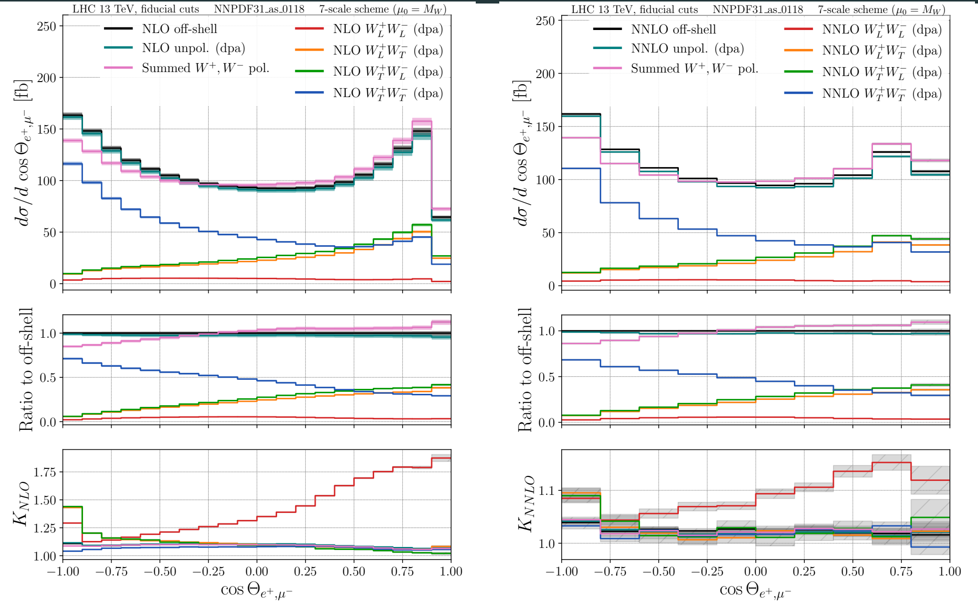

Extra figures: y_e^+

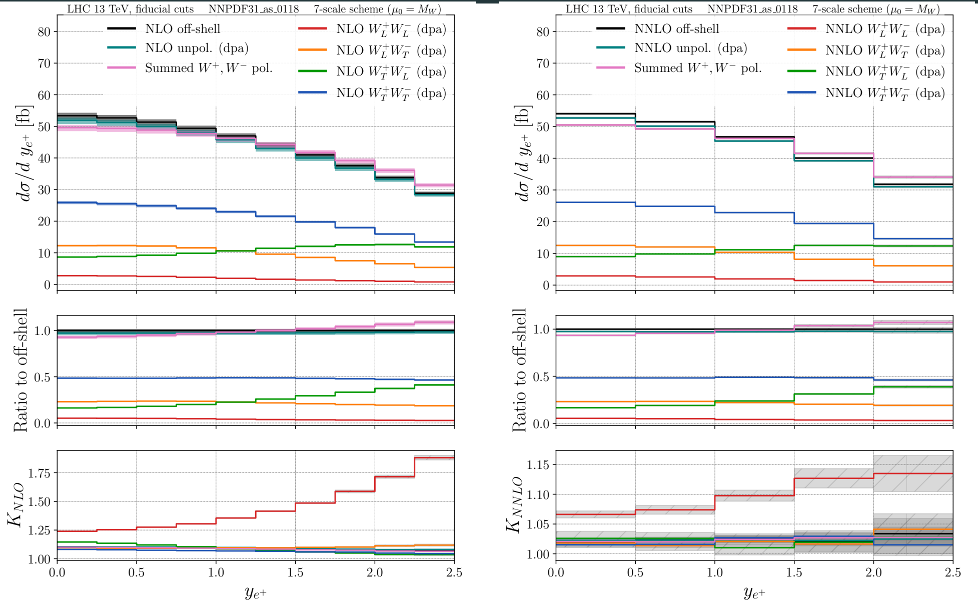

Extra figures: e^+ vs μ^-

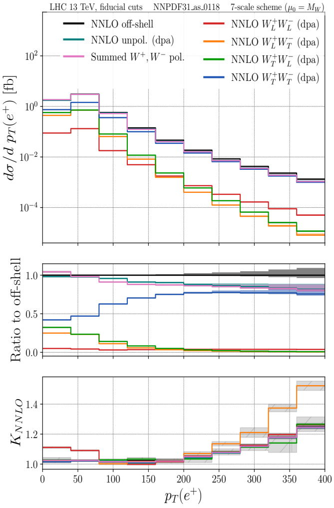

Positron transverse momentum

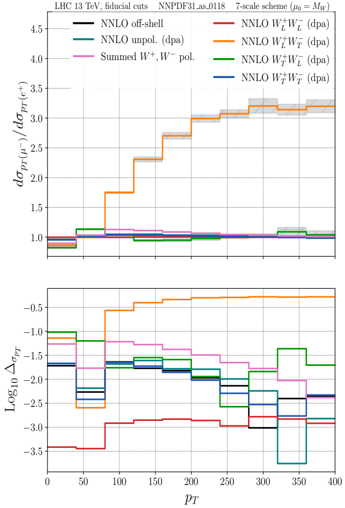

$$\log_{10}\left|\frac{\sigma_{p_T}(\mathrm{e}^+)-\sigma_{p_T}(\mu^-)}{\sigma_{p_T}(\mathrm{e}^+)+\sigma_{p_T}(\mu^-)}\right|$$

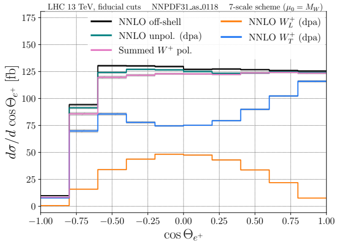

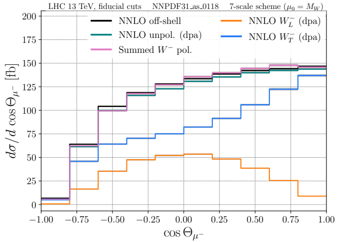

Extra figures: ϕ_{e^+,μ^-}

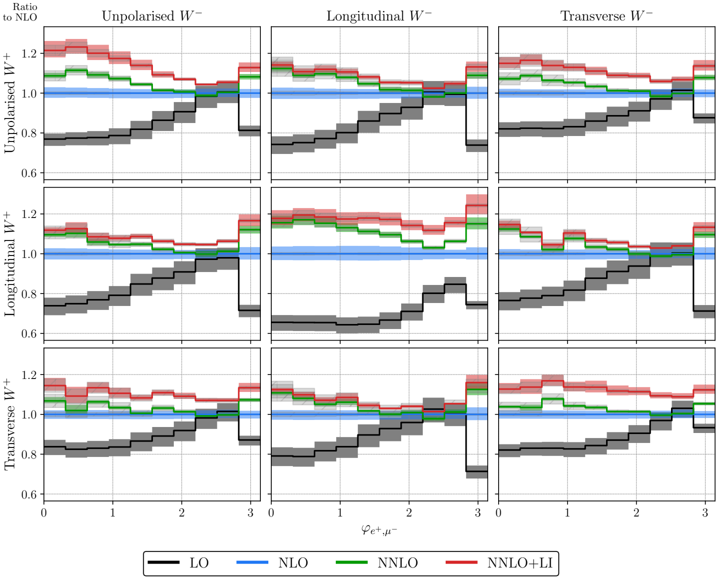

LI channel has large overall shift in TT and unpolarised setups.
Interesting shape in LL setup.

Effects of LI channel: positron transverse momentum

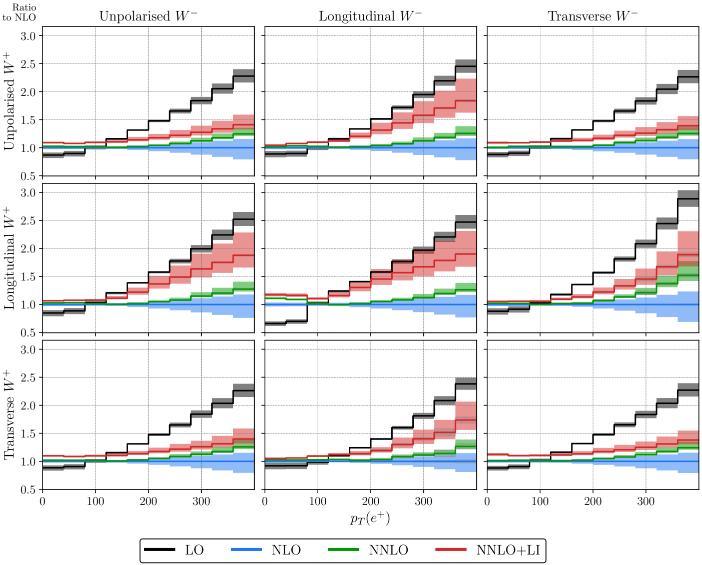

- Sizeable increase of scale uncertainty in the tail, particularly in longitudinal setups
- Corrections are polarisation-dependent:
  $\longrightarrow$ in the bulk for transverse setups
  $\longrightarrow$ in the tail for longitudinal setups
  $\longrightarrow$ in both places for LL setup